## Title
A 2n STERADIAN MAGNETIC SPECTROMETER



Authors
McReynolds, John F.
Newton, David
Wenzel, W.A.

Publication Date
1971-04-01

Submitted to Nuclear Instruments
and Methods

UCRL-20679
Preprint c.2

# A 2π STERADIAN MAGNETIC SPECTROMETER

John F. McReynolds, David Newton, and W. A. Wenzel

April 22, 1971

AEC Contract No. W-7405-eng-48

**DISCLAIMER**

# A $2\pi$ STERADIAN MAGNETIC SPECTROMETER*

John F. McReynolds, David Newton,[+] and W. A. Wenzel

Lawrence Radiation Laboratory
University of California
Berkeley, California

April 22, 1971

ABSTRACT

The magnetic properties of a $2\pi$ steradian spectrometer used in the study of $K^+$ decays at rest are described. Charged particles emitted from the axis of a cylindrically symmetric field are focussed back to the axis after one nearly circular orbit. The field has been shaped to give small spherical aberration and a relatively small overall chromatic aberration for momenta in a ten percent momentum range. Other possible experiments are described.

## I. INTRODUCTION

Magnetic spectrometers as used in the studies of nuclear $\beta$-decay have been reviewed by Siegbahn.[1] These devices differ in several important respects from spectrometers ordinarily used in high energy physics. Because of the limited strength of magnetic fields, the deflections tend to be less at high energies. The source is usually extended in three dimensions at high energies; in contrast a (solid) source of low energy $\beta$-rays must be in the form of a thin surface. The momenta of nuclear $\beta$-rays are spread over broad spectra, which are themselves matters of great interest; the decay of an elementary particle may involve only two secondaries, which are therefore monoenergetic if the decay occurs at rest. Because of their relatively



greater penetrating power, charged high energy secondaries may be exposed to more extensive measurements using relatively sophisticated detectors. In this way the particles can be identified and good momentum measurements can be made even in "bad geometry" experiments.

The spectrometer discussed here[2,3] has some characteristics of the more conventional devices used in both high energy and nuclear spectroscopy. Particles emitted on or near the axis and plane of symmetry of the cylindrically symmetric magnetic field are trapped within the field and focussed so that they return to or near the center of the magnet. As will be shown it is possible to shape the field so that monoenergetic particles from a point source are focussed into a small image whose size is determined by spherical aberrations. Alternatively it is possible to shape the field to obtain a small chromatic aberration (or final dispersion) for particles in a limited (about ten percent) momentum range. In making use of this property the distinction between the techniques of low and high energy spectroscopy are especially relevant. In nuclear spectroscopy a large final dispersion is usually essential for good resolution. For higher energy particles a small final dispersion is useful because a small detector can be used to trigger a more elaborate detection system (e.g., spark chambers) to measure the orbits at large radii, where the dispersion is maximum.

The present spectrometer was designed for an experiment to measure the branching ratio for the decay $K^+ \rightarrow e^+ + \nu$. Because this ratio is of order $10^{-5}$ a large solid angle was essential to a good event rate. At the same time, however, rejection of background demanded both good momentum resolution and the use of selective charged particle detectors. Figures 1A and 1B show the experimental arrangement. $K^+$ mesons of about 0.5 GeV/c entered along the axis of symmetry, were slowed in a beryllium or copper degrader, and stopped in a plastic target located within a gas Cherenkov counter. Secondaries were detected in scintillation counter hodoscopes, and orbits were measured using the various spark chambers. The lead cylinder terminated each orbit after a single pass.

A more detailed description of the experiment and of the detection apparatus is provided elsewhere.[3] This paper is intended to describe the properties of the spectrometer, to discuss a mathematical method for calculating field shapes which minimize aberrations, and to present other possible experimental arrangements utilizing such field shapes.

## II. ORBITS IN CYLINDRICALLY SYMMETRIC MAGNETIC FIELDS

The general properties of cylindrically symmetric magnetic fields are well known. In cylindrical coordinates r, $\theta$, z, where z is the axis of symmetry, Maxwell's equations give

$$\frac{\partial B_r}{\partial z} = \frac{\partial B_z}{\partial r} \quad \text{and} \quad \frac{\partial B_z}{\partial z} + \frac{1}{r}\frac{\partial}{\partial r}(rB_r) = 0 \qquad (1)$$

and the field components may be defined in terms of the only non-zero component ($\theta$ component) of the magnetic vector potential by

$$rB_r = \frac{-\partial}{\partial z}(rA) \quad \text{and} \quad rB_z = \frac{\partial}{\partial r}(rA) \qquad (2)$$

The field lines lie in surfaces of constant $\varphi$ ($\varphi \equiv rA$), which are therefore orthogonal to surfaces of constant magnetic scalar potential $\phi$.

The equations of motion for a particle of charge e (esu) and mass m are

$$\ddot{r} - r\dot{\theta}^2 = \frac{-e}{mc}\dot{\theta}\frac{\partial\varphi}{\partial r} \qquad (3)$$

$$\ddot{z} = \frac{-e}{mc}\dot{\theta}\frac{\partial\varphi}{\partial z} \qquad (4)$$

$$\frac{d}{dt}(mr^2\dot{\theta}) = \frac{e}{c}\cdot\frac{d\varphi}{dt} \qquad (5)$$

The last equation shows that the change in angular momentum of a particle



between two points on its orbit is proportional to the change in the value of $\varphi$ between those two points. Thus if a particle starts from the axis its angular momentum can again return to zero only if it passes through the axis again. Alternatively, the angular momentum may increase monotonically, e.g., the spiral orbit spectrometer.[4,5]

If the particle does start on the axis, (5) gives

$$r\dot{\theta} = \frac{e}{mc}A \quad \text{or} \quad mr^2\dot{\theta} = \frac{e}{c}rA \qquad (6)$$

Substituting for $\dot{\theta}$ in (3) and (4) gives

$$\ddot{r} = -\frac{e^2}{2m^2c^2}\frac{\partial A^2}{dr} \qquad (7)$$

and

$$\ddot{z} = -\frac{e^2}{2m^2c^2}\frac{\partial A^2}{dz} \qquad (8)$$

as given by Spinel and Grois.[6] The motion may therefore be described as taking place in a rotating r, z plane. In this plane there is an effective potential proportional to $A^2$, and the rotation of this plane is such as to keep the angular momentum proportional to rA.

The linear momentum and the velocity v of the particle remain constant, where

$$v^2 = \dot{r}^2 + \dot{z}^2 + r^2\dot{\theta}^2 \qquad (9)$$

Hence the maximum possible value of A is attained if $\dot{r}^2 + \dot{z}^2 = 0$, and is given by

$$A = \frac{mvc}{e} = (B\rho) \qquad (10)$$

where $(B\rho)$ is the magnetic rigidity. The minimum value of $\dot{r}^2 + \dot{z}^2$ will in general be greater than zero, and the limiting surface which contains all trajectories of given magnetic rigidity $(B\rho)$ will lie inside the surface with $A = (B\rho)$. From symmetry it is obvious that the condition that $\dot{r}^2 + \dot{z}^2 = 0$ at some point on the orbit is a sufficient condition that particles starting from the magnet center $r_o = z_o = 0$ will return through the magnet center.

From (7) and (8) the effective force in the rotating plane is in the direction of the gradient of $A^2$. Thus an orbit for which $\dot{r}^2 + \dot{z}^2$ goes to zero must appear in this rotating plane to be orthogonal to the lines of constant A in the region near its extremity. If, as is generally the case, the gradient of $A^2$ increases rapidly with radius, the maximum "force" in the (rotating) r, z plane occurs near the outer extremity of the orbit. Hence the orbit will return through the center of the magnet only if the limiting surface of constant A is essentially spherical; in the r, z plane the orbit will then be essentially a straight line. This result was first pointed out by Richardson[4] by analogy with optics; if the source and image are to be coincident they must be at the center of curvature of the "mirror" which "reflects" the rays. If the source is on the axis but not in the median plane this theorem does not strictly apply, but it is clear that for displacements $z_o$ small compared with the orbit size, focussing will occur and the image will be on the axis at a distance $z_o$ on the side of the median plane opposite to that of the source.

## III. ORBIT "STABILITY" AND DISPERSION

In practice the source of particles will not lie exactly on the axis but will extend out to some small radius $r_1$. Furthermore the momentum will not be unique but must have some spread, if only from ionization loss in leaving the source. For both these reasons there will be a spread in the maximum orbit radius $r_2$. In the design of a spectrometer, therefore, we need to consider the quantities $\left(\frac{\partial r_2}{\partial (B\rho)}\right)_{r_1}$, which is



proportional to the maximum dispersion, and $\left(\frac{\partial r_2}{\partial r_1}\right)_{(B\rho)}$, which defines the orbit stability in the sense that it is finite if neighboring orbits are bounded. Both quantities are infinite in the spiral orbit spectrometer.

For the class of spectrometers under consideration it will be sufficient to investigate the stability and dispersion of orbits in the median plane, for which, using (5), the change in the angular momentum from radius $r_1$ to $r_2$ is given by

$$(B\rho)\,(r_2 \mp r_1) = \int_{r_1}^{r_2} B_z \, r dr \tag{11}$$

The $(\mp)$ sign corresponds to the point of maximum radius being on the $\binom{\text{same}}{\text{opposite}}$ side of the magnet axis as the point of minimum radius. If $B_1$ denotes the value of $B_z$ at radius $r_1$, and $B_2$, that at radius $r_2$, then from (11)

$$\left(\frac{\partial r_2}{\partial r_1}\right)_{(B\rho)} = \frac{r_1 B_1 \mp (B\rho)}{r_2 B_2 - (B\rho)} \tag{12}$$

and

$$\left(\frac{\partial r_2}{\partial (B\rho)}\right)_{r_1} = \frac{r_2 \mp r_1}{r_2 B_2 - (B\rho)} \tag{13}$$

The orbits will therefore be "stable" provided that

$$\alpha \equiv \frac{r_2 B_2}{(B\rho)} > 1.$$

Evaluating the derivatives at $r_1 = 0$, and taking the worst case, i.e., the + sign, gives

$$\left(\frac{\partial r_2}{\partial r_1}\right)_{(B\rho)} = \frac{1}{\alpha - 1} = \frac{(B\rho)}{r_2} \left(\frac{\partial r_2}{\partial (B\rho)}\right)_{r_1 = 0} \tag{14}$$

Thus
$$\left(\frac{\partial(B\rho)}{\partial r_1}\right)_{r_2} = -\left(\frac{\partial(B\rho)}{\partial r_2}\right)_{r_1}\left(\frac{\partial r_2}{\partial r_1}\right)_{(B\rho)} = -\frac{(B\rho)}{r_2} \tag{15}$$

For a given field shape $\alpha$ can be evaluated from (11) with $r_1 = 0$. Equation (15) suggests the interesting possibility that if the momentum loss in the source is made to depend correctly on the starting position within the source, then, for particles of a given momentum, $r_2$ is independent of $r_1$. A spectrometer with this feature would necessarily give up the azimuthal symmetry which is necessary for the large aperture.

## IV. ACHROMATIC FOCUSSING

As was shown in Section II the focussing condition for particles of rigidity $(B\rho)$ is that the surface for $A = (B\rho)$ is approximately spherical. Focussing for a range of momenta therefore requires approximately spherical surfaces of constant vector potential over a range of radii. It can be seen that a field with exactly spherical surfaces of constant A everywhere does not satisfy Maxwell's equations, which imply from (1) and (2), that the function $\varphi = rA$ satisfy

$$\frac{\partial^2\varphi}{\partial z^2} + \frac{\partial^2\varphi}{dr^2} - \frac{1}{r}\frac{\partial\varphi}{\partial r} = 0. \tag{16}$$

Putting $A = A(R)$, where $R^2 = r^2 + z^2$ gives

$$\frac{\partial^2 A}{\partial R^2} + \frac{3}{R}\frac{\partial A}{\partial R} = \frac{A}{r^2} \tag{17}$$

(17) cannot be satisfied generally because the left side is a function of R only, but the right side depends on r and R.

It is useful, however, to study functional forms for fields which do satisfy Maxwell's equations and can be varied readily to make the



vector potential surfaces approximately spherical in some region. Convenient coordinates for this purpose are the dimensionless ellipsoidal parameters $\eta, \zeta$ related to r, z by

$$r/c = \sqrt{(\eta^2 - 1)(1 - \zeta^2)}\,, \qquad z/c = \eta\zeta, \tag{18}$$

where c is a scale factor.

It is shown in Lamb's book[7] that Laplace's equation is satisfied by functions of the form

$$Pn(\eta)\ Pn(\zeta),\ Pn(\eta)\ Qn(\zeta),\ Qn(\eta)\ Pn(\zeta),\ Qn(\eta)\ Qn(\zeta) \tag{19}$$

where Pn and Qn are the Legendre functions of the first and second kind. The magnetic scalar potential $\phi$ satisfies Laplace's equation, is finite at the origin and is antisymmetric about the median plane. The four functions given above therefore reduce, for a given value of n, to only one, namely, $Pn(\eta)\ Qn(\zeta)$ if n is even and $Pn(\eta)\ Pn(\zeta)$ if n is odd.

In the general expression for the magnetic scalar potential the leading term is

$$\phi_o = Po(\eta)\ Qo(\zeta) = (1/2)\ \ell n\,\frac{1+\zeta}{1-\zeta}\ \text{(focussing field)} \tag{20}$$

Particle trajectories in such a prolate spheroidal magnetic field were investigated by Richardson as a basis for a β-ray spectrometer design. In his investigations the distance of the source and image points from the median plane were not small compared with the size of the orbits, yet the acceptance solid angle was still very large compared with that of other β-ray spectrometers. The chromatic aberration unfortunately is rather large in this case.

We have investigated the correction of aberrations by adjusting the strengths of successive terms of the scalar potential

$$\phi_1 \equiv P_1(\eta)\ P_1(\zeta) = \eta\zeta = z/c \quad \text{(uniform field)}$$

$$\phi_2 \equiv P_2(\eta)\ Q_2(\zeta) = (1/2)(3\eta^2-1)\left[(1/2)(3\zeta^2-1)(1/2)\ \ln\frac{1+\zeta}{1-\zeta} - (3/2)\ \zeta\right]$$
$$\text{— (defocussing field)} \qquad (21)$$

$$\phi_3 \equiv P_3(\eta)\ P_3(\zeta) = (1/2)(5\eta^3-3\eta)(1/2)(5\zeta^3-3\zeta) \text{ — (defocussing field)}$$

The vector potential corresponding to each term of the scalar potential is given by

$$\varphi_n = \frac{c}{n\ (n+1)}\ (\eta^2-1)\ \frac{dPn(\eta)}{d\eta}\ \cdot\ (1-\zeta^2)\ \frac{dQn(\zeta)}{d\zeta} \qquad (22)$$

for $n = 0, 2, \ldots$

and

$$\varphi_n = \frac{c}{n\ (n+1)}\ (\eta^2-1)\ \frac{dPn(\eta)}{d\eta}\ \cdot\ (1-\zeta^2)\ \frac{dPn(\zeta)}{d\zeta} \qquad (23)$$

for $n = 1, 3, \ldots$

The field components are given by

$$B_z = -\frac{1}{c(\eta^2-\zeta^2)}\left[\eta(1-\zeta^2)\ \frac{\partial\phi}{\partial\zeta} + \zeta(\eta^2-1)\ \frac{\partial\phi}{\partial\eta}\right] \qquad (24)$$

and

$$B_r = \frac{\sqrt{(1-\zeta^2)\ (\eta^2-1)}}{c(\eta^2-\zeta^2)}\ \left[\zeta\frac{\partial\phi}{\partial\zeta} - \eta\frac{\partial\phi}{\partial\eta}\right]$$

We find that if the scalar potential is composed of just two terms

$$\phi = a_o\ P_o\ (\eta)\ Q_o(\zeta) + a_2\ P_2\ (\eta)\ Q_2\ (\zeta) \qquad (25)$$

where $a_o$ and $a_2$ are constants,

with $a_2 = 0.03\ a_o$, then the surfaces of constant vector potential are approximately spherical over a region with polar angle within $\pm\ 20^o$ of the median plane. Alternatively a good solution can be found using



$$\phi = a_o\ \phi_o + a_3\ \phi_3$$
$$= a_o\ P_o\ (\eta)\ Q_o\ (\zeta) + a_3\ P_3\ (\eta)\ P_3\ (\zeta) \qquad (26)$$

with $a_3 = 0.009\ a_o$. The field lines are shown in Fig. 2.

Clearly one could reduce the abberations further by including three or more values of n in the expression for $\phi$, but there does not seem to be an analytical method for finding the best amplitude for each term. Furthermore the achromatic focusing can be improved ultimately only at the expense of increased spherical aberration; hence a large aperture is available only with some compromise of the spectrometer optics. In this context a measure of the achromatic focus is the intersection (toroid of confusion) of the various orbits of momenta $p_c \pm \Delta p$ around a central momentum $p_c$.

Orbits in r—z and r—$\theta$ coordinates are shown in Fig. 3A and 3B, showing a compromise solution.(3) Solutions which emphasize small chromatic or small spherical aberrations are shown in Fig. 4A and 4B, respectively.

The detailed design of the spectrometer was carried out utilizing the LRL program CTRIM for axially symmetric magnetic fields. The magnet pole tip and coil configurations were changed until acceptable fields were calculated. The ratio of the field finally measured to that calculated differs from unity by less than .03 everywhere in the magnet volume and less than .01 over approximately 90% of the volume. Particle trajectories as measured in the various spark chambers were consistent with this level of precision.

## IV. OTHER EXPERIMENTAL APPLICATIONS IN HIGH ENERGY PHYSICS

### A. Colliding Beams

Monochromatic secondaries (from, e.g., $e^+e^- \rightarrow p^+p^-$) could be detected with scintillation counters at the outer radius of the orbit. Relatively accurate momentum determination could be made from particles passing through different sets of counters in the hodoscope as the orbit precesses around the magnet. Heavy and light secondaries could be distinguished by flight time between orbits.

### B. Missing Mass Spectrometer

Missing mass experiments such as $\pi p \rightarrow A_2 p$ could be performed with good momentum resolution for the recoil proton and downstream detectors for the multiparticle boson final states. Median plane magnetic field symmetry would be sacrificed in order to maximize aperture around a particular angle. Such a spectrometer design is shown in Fig. 5, for inner coil radius = 1 meter, central field = 18 kg, $m_{A_2}$ = 1280 MeV; $p\pi$ = 18 GeV/c, $p_o$ = 300 MeV/c, $\theta_{\pi p}$ = angle between beam and orbitting proton = $50^\circ \pm 10^\circ$. This arrangement provides a large solid angle in a selective angular range ($d\Omega$ = .25 of $4\pi$).

### C. "Precetron"

Maglic and Macek[8] have proposed to use a similar field shape at 400 kilogauss to study processes such as $\pi^+ + \pi^- \rightarrow \pi^+ + \pi^-$, $\mu^+ + \mu^- \rightarrow \mu^+ + \mu^-$ with positive and negative particles in interrotating orbits. The "magnetic bottle" would be 10 cm diameter with an angular aperture of $20^\circ$ around the median plane.



## REFERENCES

*This work was done under the auspices of the United States Atomic Energy Commission.

+Present address: University of Lancaster, England

1. Kai Siegbahn, Ed., Alpha, Beta - and Gamma-Ray Spectroscopy, North Holland Publishing Co., (1965).
2. W. A. Wenzel, LRL-Berkeley, Bevatron Report No. 953 (1967) (unpublished).
3. John F. McReynolds, Ph.D. Thesis, UCRL-20031 (1970) (unpublished).
4. H. O. W. Richardson, Phil. Mag. 40, 223 (1949); D. Michelson and H. O. W. Richardson, Proc. Phys. Soc. (London) 81, 522 (1963).
5. R. Sagane, Phys. Rev. 92, 212 (1953) and G. Iwata, G. Miyamoto, M. Kotani, UCRL translation III by Sagane and Gardener (unpublished).
6. V. S. Shpinel' and O.S. Grois, Soviet Physics, Technical Physics 1, 2191 (1956).
7. Sir Horace Lamb, Hydrodynamics, 6th edition, Cambridge University Press, pp 129-141.
8. Bogdan Maglic, Robert Macek, "Precetron, A Principle for Obtaining Pion-Pion and Muon-Muon Collisions," High Energy Physics and Nuclear Structure, pp 613-614, Devons, Samuel (ed.), New York, Plenum Press (1970).

FIGURE CAPTIONS

Fig. 1 Experimental spectrometer used to study $K^+ \rightarrow e^+ + \nu$.

a) View through median plane. O.R. means "Outer radius". The spark chambers are optical. 1 is the degrader used to stop the incident $K^+$ beam. 2 is a cylindrical scintillation counter used to detect particles penetrating the lead cylinder (4). 3 is a cylindrical spark chamber. A typical orbit is shown.

b) View through plane containing axis of symmetry. $S_2$, $S_3$, and $S_4$ are scintillation counters. A small spark chamber in the beam precedes the Cerenkov counter and stopper. The fisheyes are the first lenses in the Stereo—optical system associated with each set of outer radius spark chambers.

Fig. 2 Spectrometer coils and poletips showing a field configuration which focusses orbits at the axis.

Fig. 3 Orbits for different momenta and polar angles with field shape selected for a good overall focus.

a) r,z projection of orbits.

b) Typical orbits in r,$\theta$ projection.

Fig. 4 a) Orbits with field shape selected for an achromatic focus, showing increased spherical aberration.

b) Orbits with field shape selected for small sperical aberration, showing increased chromatic aberration.

Fig. 5 Possible magnet configuration for study of $\pi p \rightarrow A_2 p$.



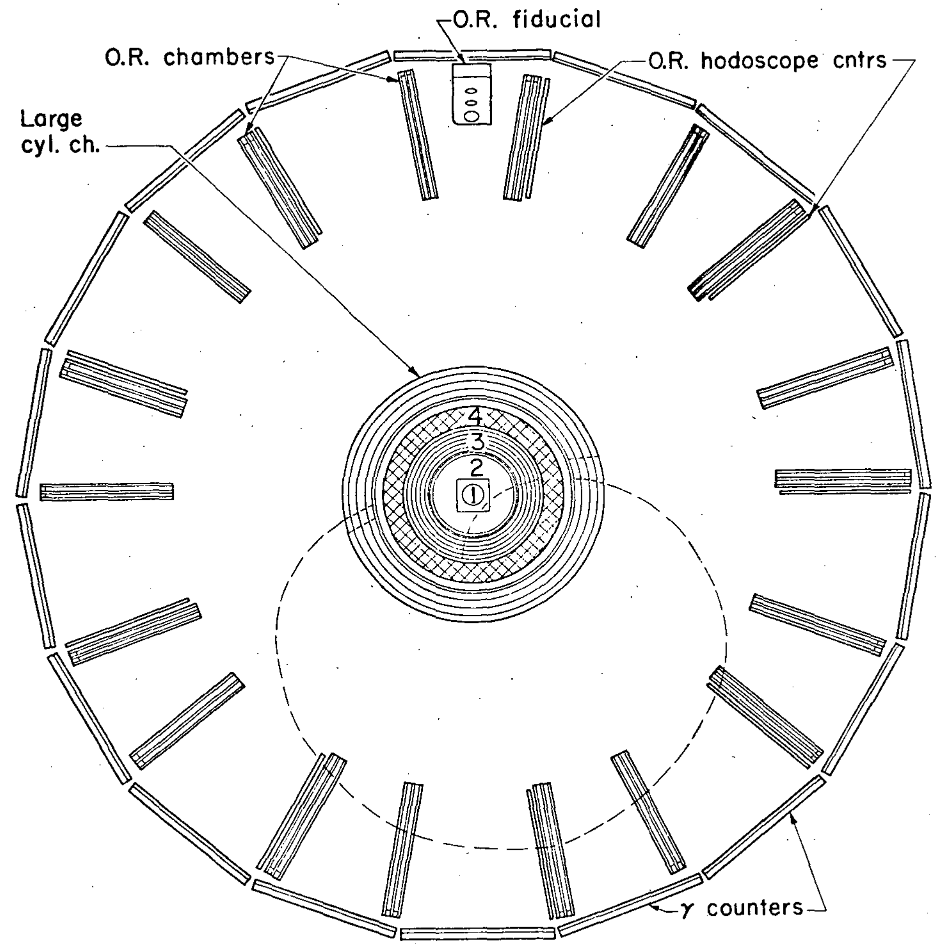


XBL708-3553

Fig. 1a

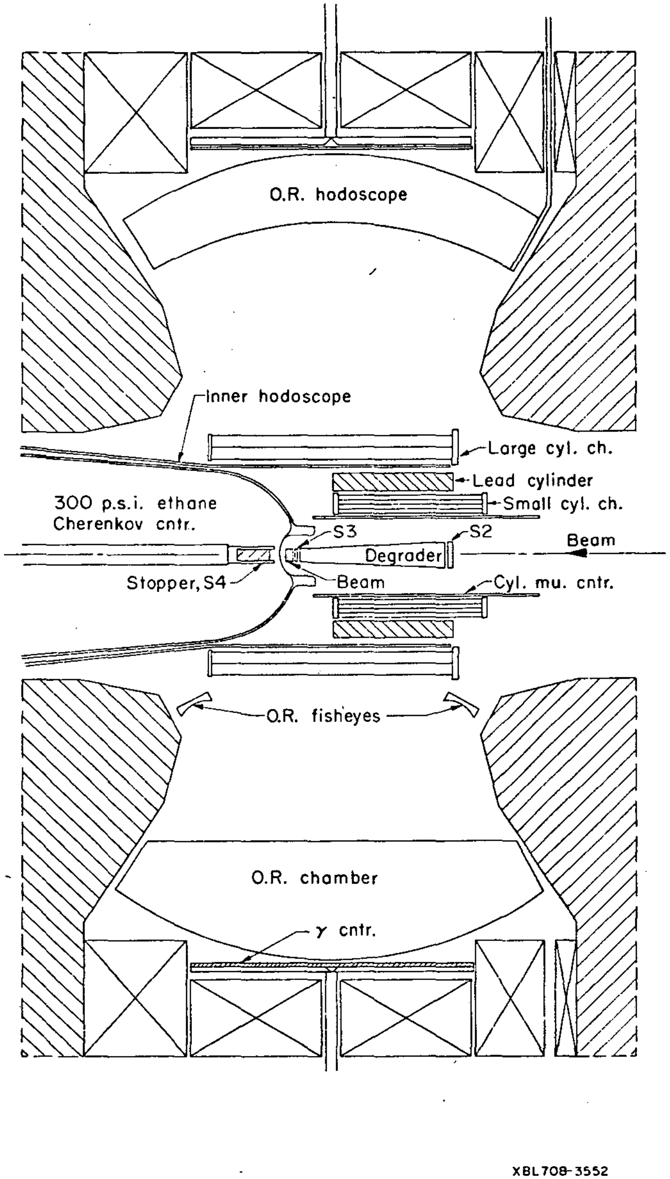
O.R. hodoscope
Inner hodoscope
Large cyl. ch.
Lead cylinder
Small cyl. ch.
300 p.s.i. ethane
Cherenkov cntr.
S3
S2
Beam
Degrader
Stopper, S4
Beam
Cyl. mu. cntr.
O.R. fisheyes
O.R. chamber
γ cntr.
XBL708-3552

Fig. 1b



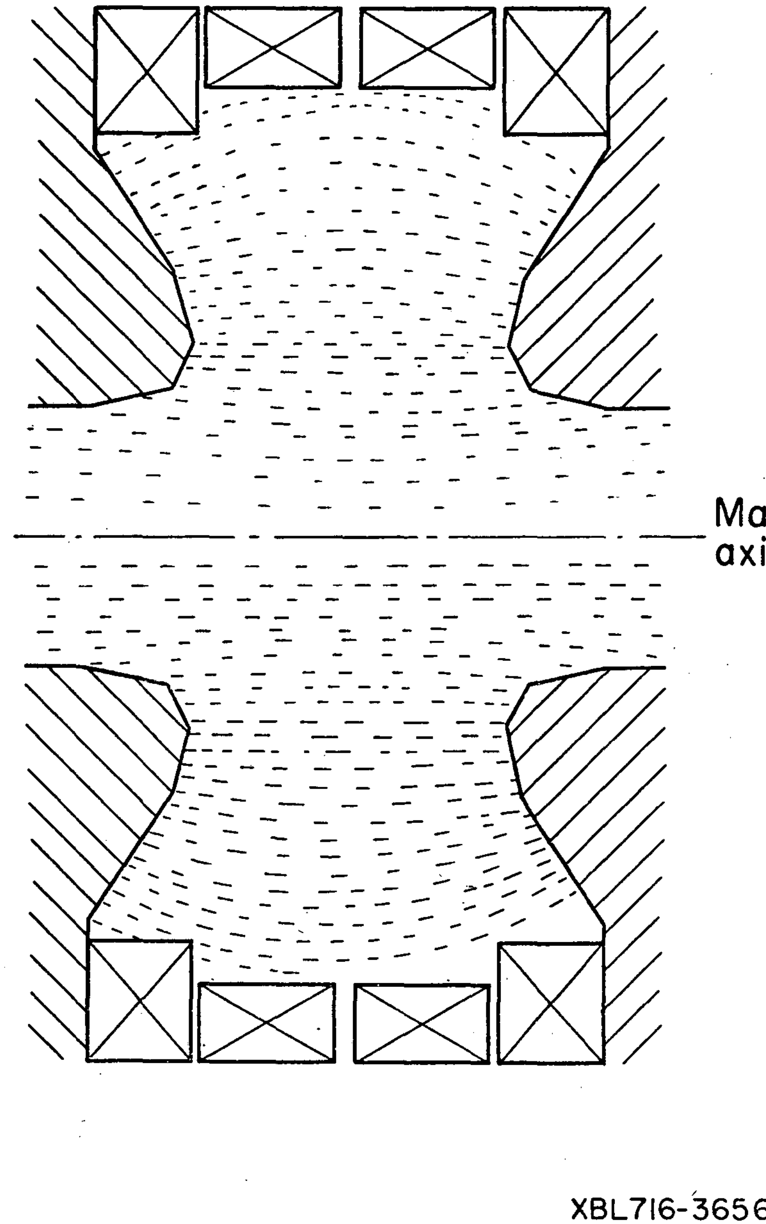
Magnet
axis
XBL716-3656

Fig. 2

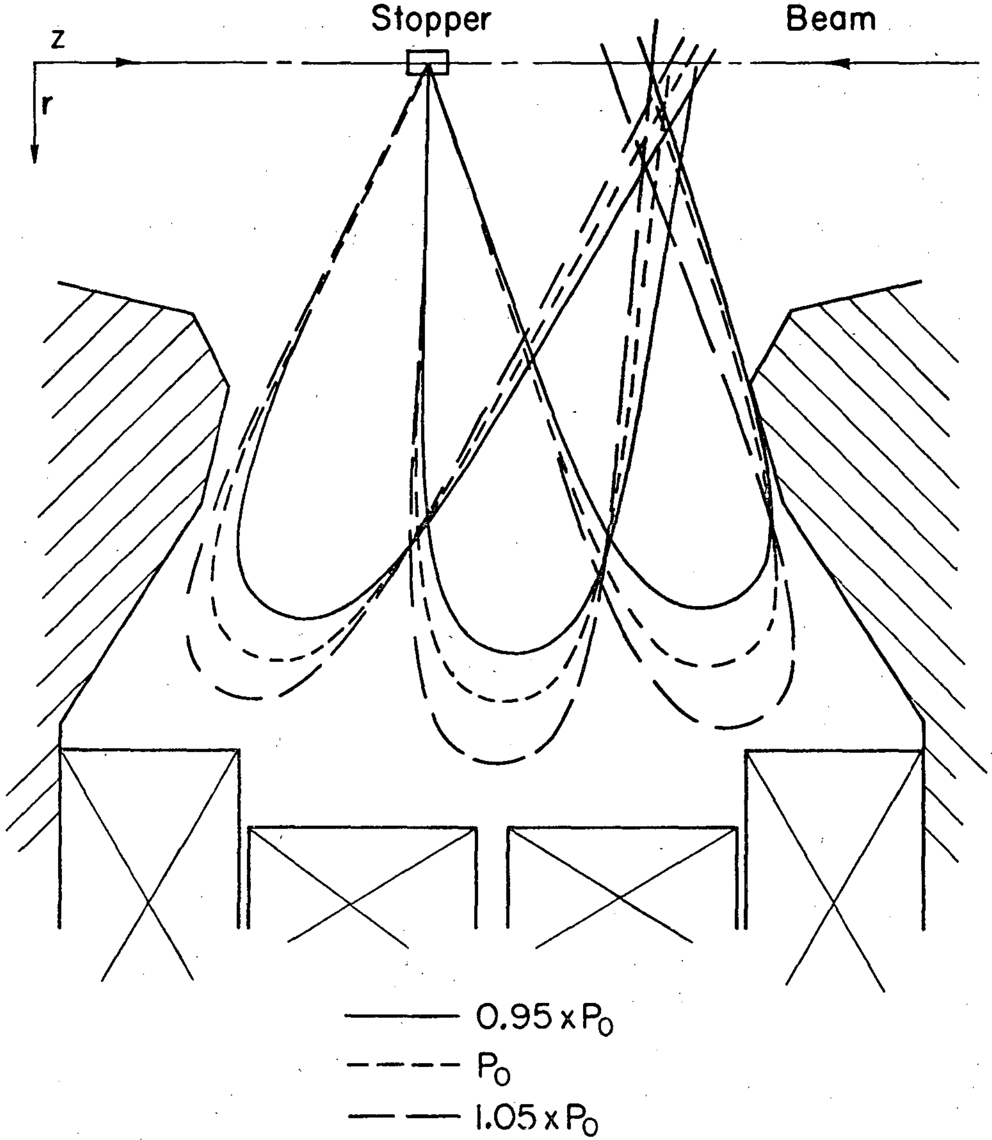
Stopper
Beam
z
r
0.95 x P0
P0
1.05 x P0
XBL716-3660

Fig. 3a



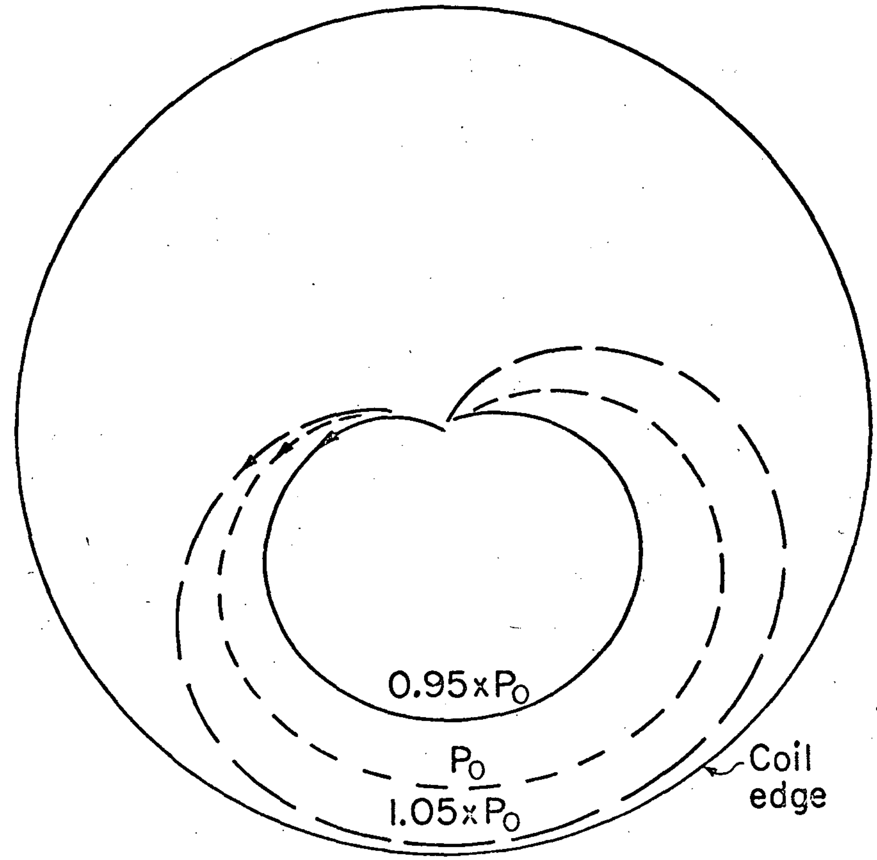
0.95 x P0
P0
1.05 x P0
Coil edge
XBL716-3667

Fig. 3b

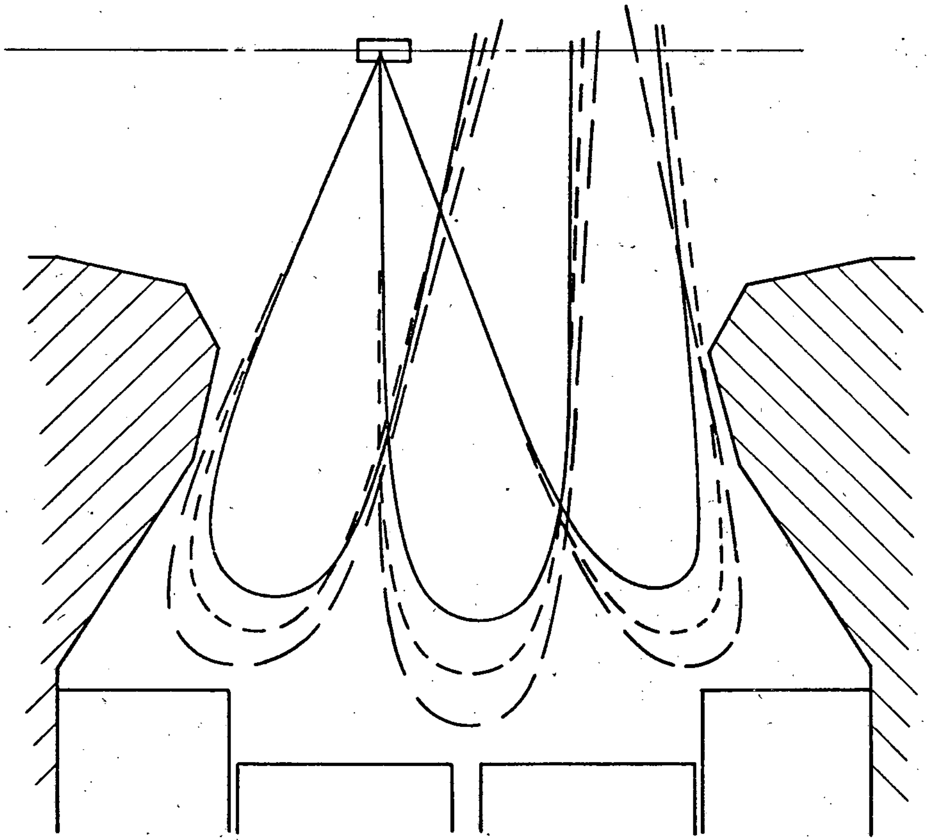

XBL716-3658

Fig. 4a



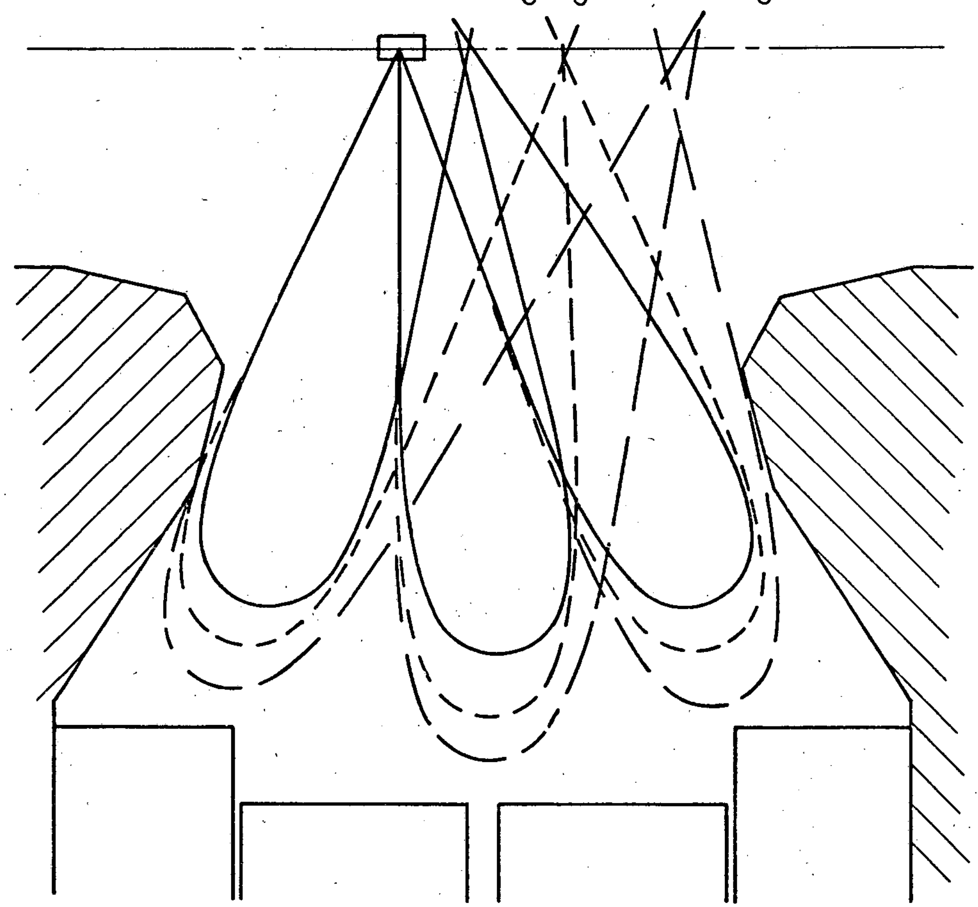


XBL 716-3657

Fig. 4b

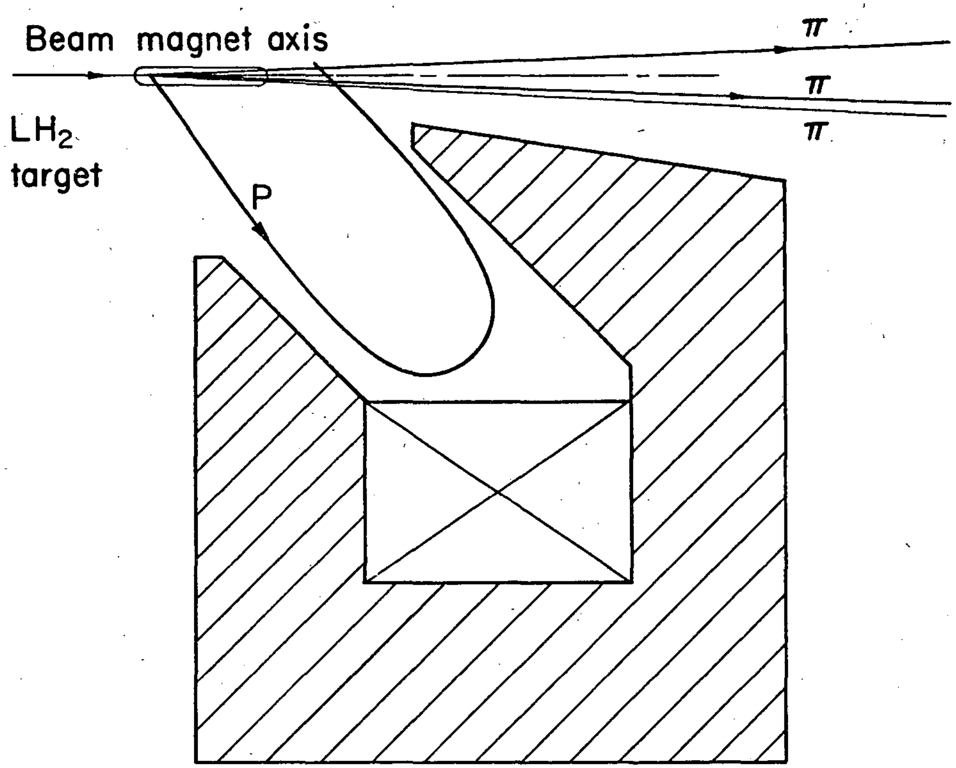


XBL716-3659

Fig. 5

TECHNICAL INFORMATION DIVISION
LAWRENCE BERKELEY LABORATORY
UNIVERSITY OF CALIFORNIA
BERKELEY, CALIFORNIA 94720